Hindawi
IET Signal Processing
Volume 2023, Article ID 8887060, 8 pages
https://doi.org/10.1049/2023/8887060

Research Article

Low-Complexity BFGS-Based Soft-Output MMSE Detector for Massive MIMO Uplink

Lin Li [1] **and Jianhao Hu** [2]

[1]*School of Physics and Electronic Information Engineering, Qinghai Normal University, Xining 810000, China*
[2]*National Key Laboratory of Science and Technology on Communications, University of Electronic Science and Technology of China, Chengdu 611731, China*

Correspondence should be addressed to Jianhao Hu; jhhu@uestc.edu.cn

Received 25 July 2023; Revised 27 September 2023; Accepted 28 October 2023; Published 14 November 2023

Academic Editor: Qinghua Guo

For the massive multiple-input multiple-output (MIMO) uplink, the linear minimum mean square error (MMSE) detector is near-optimal but involves undesirable matrix inversion. In this paper, we propose a low-complexity soft-output detector based on the simplified Broyden–Fletcher–Goldfarb–Shanno method to realize the matrix-inversion-free MMSE detection iteratively. To accelerate convergence with minimal computational overhead, an appropriate initial solution is presented leveraging the channel-hardening property of massive MIMO. Moreover, we employ a low-complexity approximated approach to calculating the log-likelihood ratios with negligible performance losses. Simulation results finally verify that the proposed detector can achieve the near-MMSE performance with a few iterations and outperforms the recently reported linear detectors in terms of lower complexity and faster convergence for the realistic massive MIMO systems.

1. Introduction

Massive multiple-input multiple-output (MIMO) has become one of the most critical techniques for future wireless communications, which promises significant improvements in data rates, spectral efficiency, and link reliability compared to the small-scale MIMO [1]. Despite these attractive benefits, the design of efficient signal detectors with high performance and low complexity presents a thorny challenge in the practical massive MIMO uplink [2].

For achieving a good trade-off between performance and complexity, linear detectors like zero-forcing and minimum mean square error (MMSE) are often resorted to. They are near-optimal with affordable complexity for massive MIMO systems, especially when the number of antennas at the base station (BS) is sufficiently large [3]. Unfortunately, the involved high-dimensional matrix inversion is complex to implement in practice [4].

To address this issue, the MMSE detector via the Neumann series expansion (NSE) is introduced in Zhang et al. [5], which employs a series of matrix-vector multiplications to approximate the matrix inversion. However, the reduced complexity is always accompanied by slow convergence. Subsequently, iterative linear detectors such as Richardson (RI) [6], conjugate gradient (CG) [7], Jacobi [8], and symmetric successive over-relaxation (SSOR) [9] are developed to accelerate convergence. Nevertheless, they all perform unsatisfactorily in the ill-conditioned propagation environments. To further enhance the detection performance, various hybrid approaches like the joint Chebyshev polynomials and SSOR (SSORCP) [10], and the fused steepest descent and nonstationary RI (SDNRI) [11] have been proposed successively but at the cost of the increased complexity.

The Broyden–Fletcher–Goldfarb–Shanno (BFGS) method as a popular quasi-Newton method is exploited in this paper to iteratively achieve the low-complexity soft-output MMSE detection without matrix inversion for the massive MIMO uplink. Leveraging the unique massive MIMO properties that the MMSE filtering matrix is Hermitian positive definite (HPD) and diagonally dominant, we provide the simplified BFGS-based MMSE detector and prove its convergence. Moreover, the involved Gram matrix computation can be circumvented by adopting matrix-vector multiplications for lower complexity. In addition, two optimization approaches, including the

selection of a proper initial solution and the approximated calculation of log-likelihood ratios (LLRs), are presented to further accelerate convergence and reduce complexity by utilizing the channel-hardening property of massive MIMO. Simulation results validate that the proposed BFGS-based detector can attain near-MMSE accuracy with a significant complexity reduction and is superior to other low-complexity linear detectors even in poor propagation environments with a high loading factor and correlated channels.

The rest of this paper is organized as follows. Section 2 briefly introduces the system model and soft-output MMSE detection. Section 3 specifies the proposed BFGS-based linear detector. Simulation results are shown in Section 4. Finally, Section 5 concludes this paper.

Notations: The bold uppercase and lowercase denote matrices and column vectors, respectively. $[\cdot]^H$, $[\cdot]^{-1}$, and $|\cdot|$ represents the conjugate transpose, inverse, and absolute operator, respectively. $\mathbb{E}\{\cdot\}$ denotes the expectation. The $K \times K$ identity matrix is denoted by $\mathbf{I}_K$.

2. Preliminaries

2.1. Uplink Massive MIMO System Model. We consider an uplink massive MIMO system employing N antennas at the BS to simultaneously serve K user antennas ($K \ll N$) with the loading factor $\beta = K/N$. The received signal vector $\mathbf{y} \in \mathbb{C}^{N\times 1}$ at the BS can be expressed by

$$\mathbf{y} = \mathbf{H}\mathbf{s} + \mathbf{n}, \tag{1}$$

where $\mathbf{H} \in \mathbb{C}^{N\times K}$ denotes the complex channel matrix. $\mathbf{s} \in \mathbb{C}^{K\times 1}$ denotes the transmitted signal vector with the average power being E_s per symbol, which is first encoded and then mapped to a constellation set Ω ($|\Omega| = 2^Q$). $\mathbf{n} \in \mathbb{C}^{N\times 1}$ denotes the complex additive white Gaussian noise vector with zero mean and N_0 variance. Without losing generality, $\mathbf{H}$ and N_0 are assumed to be perfectly known at the BS.

For realistic massive MIMO systems, the spatial correlation between signals needs to be considered, which often employs the Kronecker model [12]. Hence, the channel matrix $\mathbf{H}$ can be modeled as

$$\mathbf{H} = \mathbf{R}_B^{1/2}\mathbf{T}\mathbf{R}_U^{1/2}, \tag{2}$$

where $\mathbf{T} \in \mathbb{C}^{N\times K}$ denotes an independent and identically distributed (i.i.d.) complex Gaussian matrix with zero mean and unit variance. $\mathbf{R}_U \in \mathbb{C}^{K\times K}$ and $\mathbf{R}_B \in \mathbb{C}^{N\times N}$ denote the spatial correlation matrices at the user and BS side, respectively. The definition of $\mathbf{R}_U$ is similar to that of $\mathbf{R}_B$, and can be expressed by

$$\begin{cases} \mathbf{R}_U^{(m,k)} = (\xi_U \cdot e^{j\theta})^{k-m} \\ \mathbf{R}_U^{(k,m)} = \mathbf{R}_U^{(m,k)^*} \end{cases}, 1 \le m \le k \le K, \tag{3}$$

where ξ_U is the correlation coefficient to reflect the correlation degree among transmitting antennas and θ denotes the phase.

2.2. Soft-Output Linear MMSE Detection. For linear MMSE detection, the estimate of the transmitted signal vector $\widehat{\mathbf{s}}$ can be expressed as

$$\widehat{\mathbf{s}} = (\mathbf{H}^H\mathbf{H} + N_0E_s^{-1}\mathbf{I}_K)^{-1}\mathbf{H}^H\mathbf{y} = \mathbf{A}^{-1}\mathbf{b}, \tag{4}$$

where $\mathbf{A} = \mathbf{H}^H\mathbf{H} + N_0E_s^{-1}\mathbf{I}_K$, $\mathbf{G} = \mathbf{H}^H\mathbf{H}$, $\mathbf{b} = \mathbf{H}^H\mathbf{y}$ denote the MMSE filtering matrix, Gram matrix, and matched-filter output, respectively. Notice that $\mathbf{H}$ is column asymptotically orthogonal for massive MIMO, ensuring that $\mathbf{A}$ is HPD.

After the MMSE estimate of the transmitted signal, the soft-information LLRs can be extracted from the estimated results for the channel decoder to further improve the detection performance. Let $\mathbf{U} = \mathbf{A}^{-1}\mathbf{G}$ and $\mathbf{V} = \mathbf{U}\mathbf{A}^{-1}$, Equation (4) can be rewritten as $\widehat{\mathbf{s}} = \mathbf{U}\mathbf{s} + \mathbf{A}^{-1}\mathbf{H}^H\mathbf{n}$ combined with (1). Thus, the kth estimated symbol of $\widehat{\mathbf{s}}$ is modeled as $\widehat{s}_k = \mu_k s_k + z_k$, where $\mu_k = \mathbf{U}_{kk}$ denotes the equalized channel gain and z_k denotes the noise-plus-interference (NPI) with variance $\nu_k^2 = \mathbb{E}\{|z_k|^2\} = \sum_{m\neq k}^{K}|\mathbf{U}_{mk}|^2E_s + N_0\mathbf{V}_{kk}$. The max-log approximated LLR $L_{k,b}$ of the bit b for the kth symbol can be calculated by

$$L_{k,b} = \gamma_k\left(\min_{x\in\Omega_b^0}\left|\frac{\widehat{s}_k}{\mu_k} - x\right|^2 - \min_{x'\in\Omega_b^1}\left|\frac{\widehat{s}_k}{\mu_k} - x'\right|^2\right), \tag{5}$$

where $\gamma_k = \mu_k^2/\nu_k^2$ denotes the signal-to-interference-plus-noise ratio (SINR), and Ω_b^0, Ω_b^1 correspond to the subsets of Ω for which the bit b equals to 0 and 1, respectively.

It can be seen obviously that the matrix inversion $\mathbf{A}^{-1}$ is required by both the MMSE estimation and LLR calculation. However, the computational complexity of the exact $\mathbf{A}^{-1}$ is $\mathcal{O}(K^3)$, which always leads to high computational burden in practical massive MIMO systems.

3. Methodology

Equation (4) can be rewritten as

$$\mathbf{A}\widehat{\mathbf{s}} = \mathbf{b}. \tag{6}$$

Since $\mathbf{A}$ is HPD, finding the solution of Equation (6) is equivalent to solving a strictly convex quadratic optimization problem, that is

$$\min f(\mathbf{s}) = \frac{1}{2}\mathbf{s}^H\mathbf{A}\mathbf{s} - \mathbf{b}^H\mathbf{s}. \tag{7}$$

The quasi-Newton method [13] is widely recognized as the most efficient method to solve such kind of unconstrained optimization problems, which can be expressed in the line-search iterative form as

$$\mathbf{s}_{k+1} = \mathbf{s}_k - \alpha_k\mathbf{B}_k\mathbf{g}_k, \tag{8}$$

where α_k denotes the step size, and the search direction can be denoted by $\mathbf{d}_k = -\mathbf{B}_k\mathbf{g}_k$. Thereinto, $\mathbf{B}_k$ is a symmetric

matrix updated to approximate the Hessian inverse $\mathbf{A}^{-1}$. $\mathbf{g}_k$ is the gradient of $f(\mathbf{s})$ at $\mathbf{s}_k$ that can be calculated by $\mathbf{g}_k = \mathbf{A}\mathbf{s}_k - \mathbf{b}$.

3.1. Low-Complexity BFGS-Based Detector. As a famous quasi-Newton method, the BFGS method is utilized herein due to its numerical stability [14]. We consider the exact line search, and thus the step size needs to satisfy

$$f(\mathbf{s}_k + \alpha_k \mathbf{d}_k) = \min_{\alpha > 0} f(\mathbf{s}_k + \alpha \mathbf{d}_k). \tag{9}$$

According to $\mathbf{d}_k^H \mathbf{g}_{k+1} = 0$, we can obtain

$$\alpha_k = -\frac{\mathbf{d}_k^H \mathbf{g}_k}{\mathbf{d}_k^H \mathbf{A} \mathbf{d}_k}. \tag{10}$$

The basic idea underlying quasi-Newton methods is to obtain the advantages of Newton's method while using only the first-order information. Thus, the approximation of Hessian inverse must fulfill the following quasi-Newton condition:

$$\mathbf{B}_{k+1} \mathbf{q}_k = \mathbf{p}_k, \tag{11}$$

where $\mathbf{p}_k = \mathbf{s}_{k+1} - \mathbf{s}_k$ and $\mathbf{q}_k = \mathbf{g}_{k+1} - \mathbf{g}_k$.

For the BFGS quasi-Newton method, the approximation $\mathbf{B}_k$ to the inverse Hessian matrix is updated by

$$\begin{aligned} \mathbf{B}_{k+1} = \mathbf{B}_k &- \frac{\mathbf{p}_k \mathbf{q}_k^H \mathbf{B}_k}{\mathbf{p}_k^H \mathbf{q}_k} + \frac{\mathbf{B}_k \mathbf{q}_k \mathbf{p}_k^H}{\mathbf{p}_k^H \mathbf{q}_k} \\ &+ \left(1 + \frac{\mathbf{q}_k^H \mathbf{B}_k \mathbf{q}_k}{\mathbf{p}_k^H \mathbf{q}_k}\right) \frac{\mathbf{p}_k \mathbf{p}_k^H}{\mathbf{p}_k^T \mathbf{q}_k}. \end{aligned} \tag{12}$$

Since $\mathbf{p}_k = \mathbf{s}_{k+1} - \mathbf{s}_k = \alpha_k \mathbf{d}_k$ and $\mathbf{d}_k^H \mathbf{g}_{k+1} = 0$, we can derive $\mathbf{p}_k^H \mathbf{g}_{k+1} = 0$. Hence, we have

$$\mathbf{d}_{k+1} = -\mathbf{B}_{k+1} \mathbf{g}_{k+1} = -\mathbf{B}_k \mathbf{g}_{k+1} + \frac{\mathbf{p}_k \mathbf{q}_k^H \mathbf{B}_k}{\mathbf{p}_k^H \mathbf{q}_k} \mathbf{g}_{k+1}. \tag{13}$$

In the authors' previous work [15, 16], it has been proved that for $0 \le m \le k$,

$$\mathbf{B}_m \mathbf{g}_{k+1} = \mathbf{B}_0 \mathbf{g}_{k+1}. \tag{14}$$

Thus, Equation (13) can be simplified to

$$\mathbf{d}_{k+1} = -\mathbf{B}_0 \mathbf{g}_{k+1} + \frac{\mathbf{p}_k \mathbf{q}_k^H \mathbf{B}_0}{\mathbf{p}_k^H \mathbf{q}_k} \mathbf{g}_{k+1}. \tag{15}$$

Notice that $\mathbf{B}_0$ is always initialized as a simple HPD matrix, which can be set as an identity matrix herein for further lower complexity. Hence, we have

$$\begin{aligned} \mathbf{d}_{k+1} &= -\mathbf{g}_{k+1} + \frac{\mathbf{p}_k \mathbf{q}_k^H}{\mathbf{p}_k^H \mathbf{q}_k} \mathbf{g}_{k+1} \\ &= -\left(\mathbf{I}_K - \frac{\mathbf{p}_k \mathbf{q}_k^H}{\mathbf{p}_k^H \mathbf{q}_k}\right) \mathbf{g}_{k+1}. \end{aligned} \tag{16}$$

Suppose

$$\mathbf{S}_{k+1} = \mathbf{I}_K - \frac{\mathbf{p}_k \mathbf{q}_k^H}{\mathbf{p}_k^H \mathbf{q}_k}, \tag{17}$$

we can obtain $\mathbf{d}_{k+1} = -\mathbf{S}_{k+1} \mathbf{g}_{k+1}$, which is similar to the search direction of the traditional BFGS method but with significant complexity reduction. In addition, by adding an extra term $-\frac{\mathbf{q}_k \mathbf{p}_k^H}{\mathbf{p}_k^H \mathbf{q}_k}$, $\mathbf{S}_{k+1}$ can be transformed into a HPD matrix without changing the search direction.

3.2. Initial Solution Selection. Consider the selection of an initial solution, which is generally set to a zero vector if no prior information about the exact solution can be obtained. In practice, the initial solution often plays an essential role in the convergence rate, thus affecting the complexity and accuracy. An initial solution close to the final solution will lead to fewer iterations. Therefore, it is of great significance to select an appropriate initial solution.

For massive MIMO systems, the column vectors of the channel matrix $\mathbf{H}$ are asymptotically orthogonal when $N \gg K$, that is

$$\mathbf{h}_i^H \frac{\mathbf{h}_j}{N} \to 0, \ i \ne j, \ i, j = 1, 2, \cdots, K, \tag{18}$$

where $\mathbf{h}_i$ is the ith column vector of $\mathbf{H}$. Thus the Gram matrix $\mathbf{G}$ and filtering matrix $\mathbf{A}$ are diagonally dominant especially when the loading factor is small [17]. Leveraging the special massive MIMO properties described above, a low-complexity initial solution is proposed as

$$\mathbf{s}_0 = N^{-1} \mathbf{b}. \tag{19}$$

Therefore, since the diagonal-approximate initial solution more closer to the final solution than the zero-vector initial solution, the proposed BFGS-based detector can achieve a more rapid convergence rate. Moreover, such a hardware-friendly initialization way adds very little computation.

3.3. Approximated LLR Calculation. Although the proposed BFGS-based detector can circumvent the exact calculation of $\mathbf{A}^{-1}$ required by MMSE detection, the LLR calculation mentioned previously still needs to calculate $\mathbf{A}^{-1}$. To address this issue, we provide an approximated LLR calculation approach to calculating the channel gain and NPI variance inspired by Dai et al. [18].

According to the diagonally dominant property of the MMSE filtering matrix $\mathbf{A}^{-1}$, we can rewrite the equalized channel matrix as

$$\mathbf{U} = \mathbf{I}_K - N_0 E_s^{-1}\mathbf{A}^{-1} \approx \frac{N}{N + N_0 E_s^{-1}}\mathbf{I}_K, \tag{20}$$

that is, the inverse of the equalized channel gain can be approximated as

$$\mu_k^{-1} \approx 1 + \frac{N_0 E_s^{-1}}{N}. \tag{21}$$

Following Liu et al. [19], the NPI variance can be calculated as

$$\nu_k^2 = E_s \mu_k (1 - \mu_k). \tag{22}$$

Thus, the posteriori SINR can be given by

$$\gamma_k = \frac{1}{E_s\left(\mu_k^{-1} - 1\right)} \approx \frac{N}{N_0}. \tag{23}$$

We can see obviously that the complexity can be greatly reduced by utilizing Equations (21) and (23) to approach the exact LLR calculation. In summary, the proposed low-complexity BFGS-based iterative detector for achieving the soft-output MMSE detection is shown in Algorithm 1.

It's worth pointing out that we can change the calculation in line 8 to $\mathbf{A}\mathbf{d}_k = \mathbf{H}^H(\mathbf{H}\mathbf{d}_k) + \lambda\mathbf{d}_k$, which can also save the complex Gram matrix calculation required by the MMSE filtering matrix $\mathbf{A}$ in the preprocessing step. Hence, the proposed BFGS-based detector can be flexibly adapted to various propagation environments for lower complexity.

3.4. Convergence Analysis. We focus on the convergence rate of the proposed BFGS-based iterative detector in this subsection. Let $\mathbf{s}^*$ be the unique minimum point of f, and utilize the $\mathbf{A}$-norm of the error vector $\mathbf{e}_k = \mathbf{s}_k - \mathbf{s}^*$ to evaluate the convergence rate.

We first expand the square of the $\mathbf{A}$-norm of $\mathbf{e}_{k+1} = \mathbf{e}_k + \alpha_k\mathbf{d}_k$ as

$$\|\mathbf{e}_{k+1}\|_A^2 = (\mathbf{A}\mathbf{e}_{k+1}, \mathbf{e}_k) - \alpha_k(\mathbf{A}\mathbf{e}_{k+1}, \mathbf{d}_k). \tag{24}$$

Since $\mathbf{s}^* = \mathbf{A}^{-1}\mathbf{b}$, we can get $\mathbf{A}\mathbf{e}_{k+1} = \mathbf{A}\mathbf{s}_{k+1} - \mathbf{b} = \mathbf{g}_{k+1}$, and thus $(\mathbf{A}\mathbf{e}_{k+1}, \mathbf{d}_k) = 0$ referring to the exact line search.

Combined with $\mathbf{d}_k = -\mathbf{S}_k\mathbf{g}_k$, we derive that

$$\begin{aligned}
\|\mathbf{e}_{k+1}\|_A^2 &= (\mathbf{A}\mathbf{e}_k, \mathbf{e}_k) + \alpha_k(\mathbf{A}\mathbf{d}_k, \mathbf{e}_k) \\
&= \|\mathbf{e}_k\|_A^2 + \alpha_k(\mathbf{d}_k, \mathbf{g}_k) \\
&= \|\mathbf{e}_k\|_A^2\left(1 - \frac{(\mathbf{d}_k, \mathbf{g}_k)^2}{(\mathbf{A}\mathbf{d}_k, \mathbf{d}_k)(\mathbf{A}^{-1}\mathbf{g}_k, \mathbf{g}_k)}\right) \\
&= \|\mathbf{e}_k\|_A^2\left(1 - \frac{\left(\mathbf{g}_k^H\mathbf{S}_k\mathbf{g}_k\right)^2}{\left(\mathbf{g}_k^H\mathbf{S}_k\mathbf{A}\mathbf{S}_k\mathbf{g}_k\right)\left(\mathbf{g}_k^H\mathbf{A}^{-1}\mathbf{g}_k\right)}\right).
\end{aligned} \tag{25}$$

Assuming $\mathbf{Q}_k = \mathbf{S}_k^{1/2}\mathbf{A}\mathbf{S}_k^{1/2}$ and $\mathbf{x}_k = \mathbf{S}_k^{1/2}\mathbf{g}_k$, we have $\frac{\left(\mathbf{g}_k^H\mathbf{S}_k\mathbf{g}_k\right)^2}{\left(\mathbf{g}_k^H\mathbf{S}_k\mathbf{A}\mathbf{S}_k\mathbf{g}_k\right)\left(\mathbf{g}_k^H\mathbf{A}^{-1}\mathbf{g}_k\right)} = \frac{\left(\mathbf{x}_k^H\mathbf{x}_k\right)^2}{\left(\mathbf{x}_k^H\mathbf{Q}_k\mathbf{x}_k\right)\left(\mathbf{x}_k^H\mathbf{Q}_k^{-1}\mathbf{x}_k\right)}$. By applying the Kantorovich inequality [20], we finally obtain

Input: $\mathbf{H}$, $\mathbf{y}$, N_0, E_s;
Output: LLRs;
1 **Preprocessing:**
2 $\mathbf{b} = \mathbf{H}^H\mathbf{y}$, $\lambda = N_0E_s^{-1}$,
3 $\mathbf{A} = \mathbf{H}^H\mathbf{H} + \lambda\mathbf{I}_K$;
4 **Initialization:**
5 $\mathbf{s}_0 = N^{-1}\mathbf{b}$, $\mathbf{g}_0 = \mathbf{A}\mathbf{s}_0 - \mathbf{b}$, $\mathbf{d}_0 = -\mathbf{g}_0$;
6 **Iteration:**
7 **for** $k = 0, \cdots, maxIter - 1$ **do**
8 $\quad\mathbf{r}_k = \mathbf{A}\mathbf{d}_k$;
9 $\quad\alpha_k = -\frac{\mathbf{d}_k^H\mathbf{g}_k}{\mathbf{d}_k^H\mathbf{r}_k}$;
10 $\quad\mathbf{p}_k = \alpha_k\mathbf{d}_k$, $\mathbf{q}_k = \alpha_k\mathbf{r}_k$;
11 $\quad\mathbf{s}_{k+1} = \mathbf{s}_k + \mathbf{p}_k$;
12 $\quad\mathbf{g}_{k+1} = \mathbf{g}_k + \mathbf{q}_k$;
13 $\quad\mathbf{d}_{k+1} = -\mathbf{g}_{k+1} + \frac{\mathbf{p}_k\mathbf{q}_k^H\mathbf{g}_{k+1}}{\mathbf{p}_k^H\mathbf{q}_k}$;
14 **end**
15 $\widehat{\mathbf{s}} = \mathbf{s}_{k+1}$;
16 **LLR calculation:**
17 $\mu_k^{-1} \approx 1 + \frac{\lambda}{N}$;
18 $\gamma_k = \frac{N}{N_0}$;
19 **for** $k = 1, \cdots, K$ **do**
20 $\quad$**for** $b = 1, \cdots, Q$ **do**
21 $\quad\quad\psi_{k,b} = \left(\min_{x\in\Omega_b^0}\left|\frac{\widehat{s}_k}{\mu_k} - x\right|^2 - \min_{x'\in\Omega_b^1}\left|\frac{\widehat{s}_k}{\mu_k} - x'\right|^2\right)$;
22 $\quad\quad L_{k,b} = \gamma_k\psi_{k,b}$.
23 $\quad$**end**
24 **end**

Algorithm 1: Proposed BFGS-based detector.

$$\|\mathbf{e}_{k+1}\|_A^2 \leqslant \left(\frac{C_k - c_k}{C_k + c_k}\right)^2\|\mathbf{e}_k\|_A^2, \tag{26}$$

where C_k and c_k are, respectively, the largest and smallest eigenvalues for $\mathbf{Q}_k$. Due to that $\mathbf{S}_k^{1/2}\mathbf{Q}_k\mathbf{S}_k^{-1/2} = \mathbf{S}_k\mathbf{A}$, we see that $\mathbf{S}_k\mathbf{A}$ is similar $\mathbf{Q}_k$ with the same eigenvalues.

Therefore, the convergence of the proposed BFGS-based detector can be guaranteed. Moreover, if $\mathbf{S}_k^{-1}$ is close to $\mathbf{A}$, both c_k and C_k will be close to unity leading to the rapid convergence rate.

4. Simulation Results

In this section, the simulation results of BER performance versus different SNRs and the numerical comparison of computational complexity are provided to verify the effectiveness of the proposed BFGS-based detector compared to other conventional linear detectors. The performance of the exact MMSE detector is included as the benchmark for comparison. Rate-0.5 convolutional code with $[133_o, 171_o]$ polynomial and 64-QAM modulation are employed in all simulations.

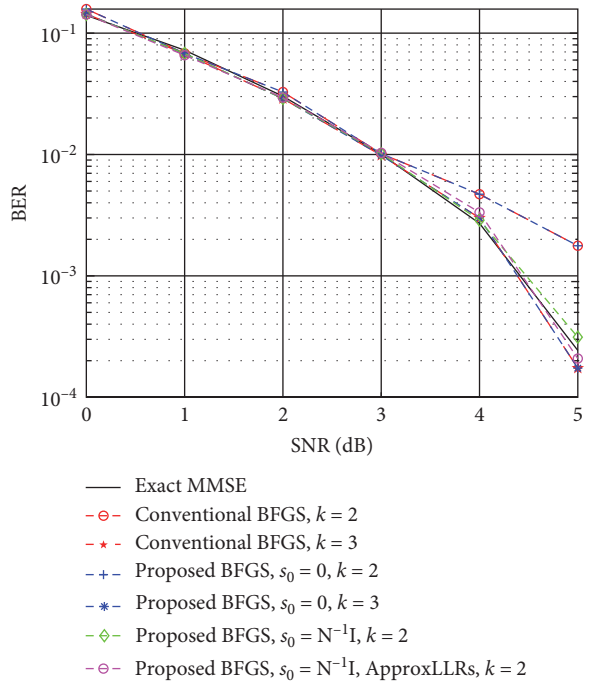

Figure 1: BER performance of the proposed detector in i.i.d. Rayleigh fading channels with 128×8 antenna configuration.

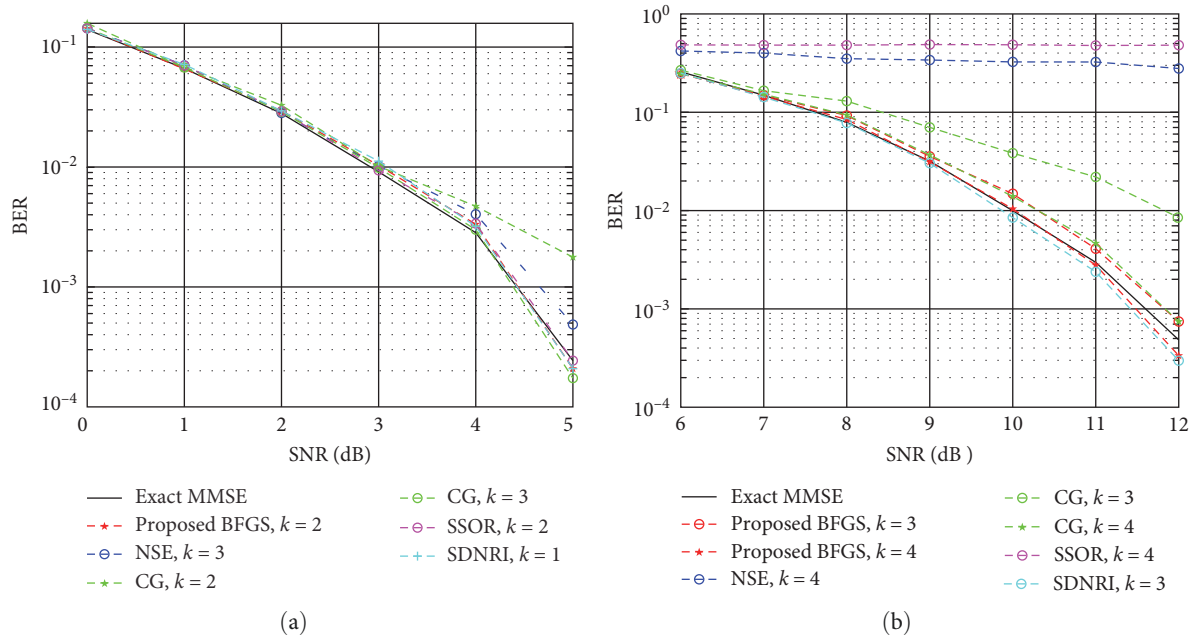

Figure 2: Performance comparison of the proposed detector with other detectors in i.i.d. Rayleigh fading channels with different antenna configurations. (a) 8×128 and (b) 32×128.

4.1. BER Performance. Figure 1 shows the BER performance evaluation of the proposed BFGS-based detector in i.i.d. Rayleigh fading channels with 128×8 antenna configuration. We can see that the performance of the simplified BFGS-based detector without initialization is identical to that of the conventional BFGS-based detector as we analyzed in Section 3.1. Moreover, the different number of iterations exhibits the proposed BFGS-based detector with the initial solution $\mathbf{s}_0 = N^{-1}\mathbf{b}$ can achieve rapid convergence rate. Besides, the performance of the proposed BFGS-based detector with the approximated LLR calculation is very close to the performance of the exact MMSE detector, which illustrates the effectiveness of the proposed detector in typical massive MIMO systems.

Figure 2 provides the BER performance comparison of the proposed BFGS-based detector with the existing low-complexity linear detectors (namely, NSE, CG, SSOR, SDNRI) in i.i.d. Rayleigh fading channels with 128×8 and 128×32 antenna configurations, respectively. It first can be seen that the proposed

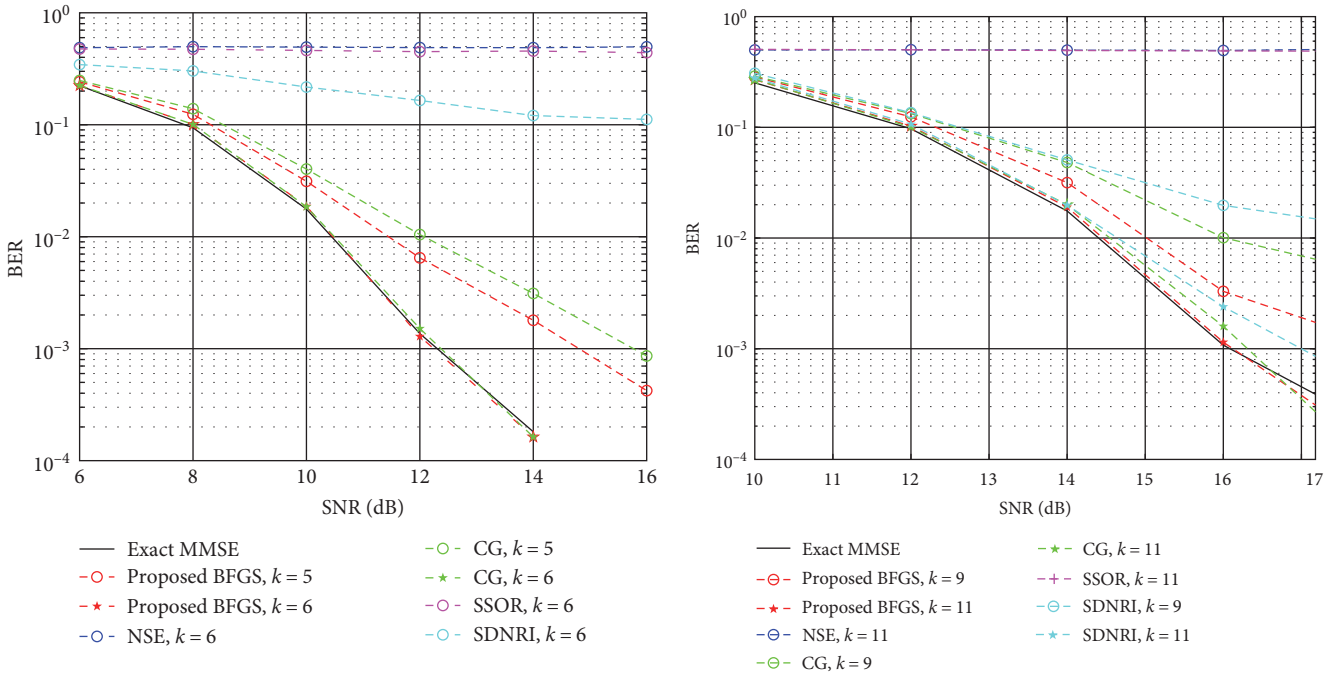

Figure 3: Performance comparison of the proposed detector with other detectors in spatially correlated channels with different antenna configurations. (a) 8×128, $\xi_B = \xi_U = 0.8$ and (b) 32×128, $\xi_B = \xi_U = 0.6$.

BFGS-based detector achieves near-MMSE detection performance with a small number of iterations for both the two different antenna configurations. NSE-based and SSOR-based detectors both perform well under the antenna configuration with the small loading factor but do not work in the big loading factor case. Compared with the proposed BFGS-based detector, CG-based detector converges slower while SDNRI-based detector converges faster. However, notice that SDNRI adopts the hybrid approach, which is more complex at each iteration correspondingly.

We compare the BER performance of the proposed BFGS-based detector with that of the other low-complexity linear detectors mentioned above in the spatially correlated channels with 128×8 and 128×32 antenna configurations in Figure 3. The correlation coefficients ξ_B and ξ_U reflect the degree of the channel correlation. The greater the channel correlation coefficient, the higher the channel correlation and the worse the propagation environment. On the whole, the channel correlation will lead to slow convergence of the iterative detectors under the same antenna configuration. We can observe that NSE-based and SSOR-based still perform worst in the poor propagation environments. Although SDNRI-based detector works well in i.i.d. Rayleigh fading channels but it converges very slowly when the channel correlation is increased. Compared to other low-complexity linear iterative detectors, the proposed BFGS-based detector performs satisfactorily in such ill-conditioned propagation cases with a great loading factor and correlated channels.

4.2. Complexity Comparison. We analyze the computational complexity through the required number of complex-valued multiplications. The total complexity mainly comes from the preprocessing step and iteration process. In general, the preprocessing includes the calculation of the matrix $\mathbf{A}$ and the vector $\mathbf{b}$ as shown in Algorithm 1, which requires $NK^2 + NK$ multiplications. The NSE-based CG-based, and SSOR-based detectors all share such preprocessing complexity. Notice that the Gram matrix computation-free detectors like the SDNRI-based detector do not require the preprocessing step. Besides, the proposed BFGS1-based detector corresponds to Algorithm 1 requiring the preprocessing, while the proposed BFGS2-based detector adopts matrix-vector multiplications to avoid the Gram matrix computation.

Table 1: Comparison of computational complexity.

Detectors	Number of multiplications
NSE [5]	$2K^2 - 2K + (L-2)K^3$ $(L>2)$
SSOR [9]	$(4K^2 + 4K)L$
CG [7]	$(2K^2 + 7K)L$
SDNRI [11]	$(4NK + 7K)L$
Conventional BFGS	$(7K^2 + 7K)L$
Proposed BFGS1	$(K^2 + 5K)L$
Proposed BFGS2	$(2NK + 7K)L$

The complexity of the aforementioned iterative detectors at each iteration is presented in Table 1. Thereinto, L denotes the number of iterations. It can be seen that the proposed BFGS-based detector significantly reduces the complexity of the conventional BFGS method for MMSE detection. Moreover, we can observe that it has lower complexity compared with other typical low-complexity linear detectors.

Table 2: Number of complex-valued multiplications.

Detectors	Multiplications with L in Figure 3(b)
Cholesky	202,752 (100%)
NSE	432,064 (213.1%)
SSOR	181,632 (89.6%)
CG	160,160 (79.0%)
SDNRI	182,688 (90.0%)
Conventional BFGS	216,480 (106.8%)
Proposed BFGS1	148,192 (73.1%)
Proposed BFGS2	92,576 (45.7%)

The total complexity evaluation of the discussed iterative detectors is specified in Table 2. As can be clearly seen from the above performance simulation, the proposed detector performs best in the propagation cases with large loading factor and correlated channels. Thus, we evaluate the complexity comparison with the simulated number of iterations in Figure 3(b) accordingly. The multiplications of the exact Cholesky-based MMSE detection are included as a baseline for comparison. It can be seen that the proposed BFGS-based detector has the lowest complexity while attaining the best performance compared with the other linear detectors. Thus, we can conclude that the proposed detector achieves a better performance and complexity trade-off.

5. Conclusion

In this paper, we propose a simplified BFGS method to iteratively realize the massive MIMO MMSE detection without matrix inversion, which is identical to the conventional BFGS method theoretically but reduces the complexity significantly. The convergence analysis of the proposed BFGS method is also provided. By fully utilizing the special properties of massive MIMO that the MMSE filtering matrix is diagonally dominant, the efficient initial solution and approximated LLR calculation are further proposed to enhance the detection performance in terms of the convergence rate and computational complexity. In addition, the Gram matrix computation can be transformed into the matrix-vector multiplications for lower complexity. Numerical results demonstrate that the proposed BFGS-based soft-output detector can achieve near-MMSE performance with a few iterations and is superior to other typical low-complexity linear detectors, especially in poor propagation environments. Future works will focus on the hybrid approaches based on the proposed BFGS method and then the efficient design of the corresponding hardware architecture.

Data Availability

No underlying data was collected or produced in this study.

Conflicts of Interest

The authors declare that they have no conflicts of interest.

References

[1] E. G. Larsson, O. Edfors, F. Tufvesson, and T. L. Marzetta, "Massive MIMO for next generation wireless systems," *IEEE Communications Magazine*, vol. 52, no. 2, pp. 186–195, 2014.

[2] L. Lu, G. Y. Li, A. L. Swindlehurst, A. Ashikhmin, and R. Zhang, "An overview of massive MIMO: benefits and challenges," *IEEE Journal of Selected Topics in Signal Processing*, vol. 8, no. 5, pp. 742–758, 2014.

[3] S. Yang and L. Hanzo, "Fifty years of MIMO detection: the road to large-scale MIMOs," *IEEE Communications Surveys & Tutorials*, vol. 17, no. 4, pp. 1941–1988, 2017.

[4] M. A. Albreem, W. Salah, A. Kumar et al., "Low complexity linear detectors for massive MIMO: a comparative study," *IEEE Access*, vol. 9, pp. 45740–45753, 2021.

[5] X. Zhang, H. Zeng, B. Ji, and G. Zhang, "Low-complexity implicit detection for massive MIMO using Neumann series," *IEEE Transactions on Vehicular Technology*, vol. 71, no. 8, pp. 9044–9049, 2022.

[6] I. A. Khoso, X. Zhang, and A. H. Shaikh, "Low-complexity signal detection for large-scale MIMO systems with second-order Richardson method," *Electronics Letters*, vol. 56, no. 9, pp. 467–469, 2020.

[7] S. Berthe, X. Jing, H. Liu, and Q. Chen, "Low-complexity soft-output signal detector based on adaptive pre-conditioned gradient descent method for uplink multiuser massive MIMO systems," *Digital Communications and Networks*, vol. 9, no. 2, pp. 557–566, 2023.

[8] P. Chan-Yeob, H.-R. Jae, J.-Y. Jang, and S. Hyoung-Kyu, "An enhanced Jacobi precoder for downlink massive MIMO systems," *Computers, Materials and Continua*, vol. 68, no. 1, pp. 137–148, 2021.

[9] S. Berthe, X. Jing, R. Tang, H. Liu, and Q. Chen, "Low-complexity soft-output signal detector based on AI-SSOR preconditioned conjugate gradient method over massive MIMO correlated channel," *Physical Communication*, vol. 56, Article ID 101948, 2023.

[10] Q. Deng, L. Guo, C. Dong, X. Liang, and J. Lin, "Hybrid iterative updates detection scheme for uplink dynamic multiuser massive MIMO systems," in *2017 IEEE Globecom Workshops (GC Wkshps)*, IEEE, 2017.

[11] I. A. Khoso, X. Zhang, X. Dai, A. Ahmed, and Z. A. Dayo, "Joint steepest descent and non-stationary Richardson method for low-complexity detection in massive MIMO systems," *Transactions on Emerging Telecommunications Technologies*, vol. 33, no. 9, Article ID e4566, 2022.

[12] B. E. Godana and T. Ekman, "Parametrization based limited feedback design for correlated MIMO channels using new statistical models," *IEEE Transactions on Wireless Communications*, vol. 12, no. 10, pp. 5172–5184, 2013.

[13] J. Nocedal and S. J. Wright, "Large-scale unconstrained optimization," in *Numerical Optimization*, pp. 164–192, Springer, 2006.

[14] Z. Wei, G. Yu, G. Yuan, and Z. Lian, "The superlinear convergence of a modified BFGS-type method for unconstrained optimization," *Computational Optimization and Applications*, vol. 29, no. 3, pp. 315–332, 2004.

[15] L. Li and J. Hu, "An efficient linear detection scheme based on L-BFGS method for massive MIMO systems," *IEEE Communications Letters*, vol. 26, no. 1, pp. 138–142, 2022.

[16] L. Li and J. Hu, "Fast-converging and low-complexity linear massive MIMO detection with L-BFGS method," *IEEE Transactions on Vehicular Technology*, vol. 71, no. 10, pp. 10656–10665, 2022.

[17] F. Rusek, D. Persson, B. K. Lau et al., "Scaling up MIMO: opportunities and challenges with very large arrays," *IEEE Signal Processing Magazine*, vol. 30, no. 1, pp. 40–60, 2013.
[18] L. Dai, X. Gao, X. Su, S. Han, I. Chih-Lin, and Z. Wang, "Low-complexity soft-output signal detection based on Gauss–Seidel method for uplink multiuser large-scale MIMO systems," *IEEE Transactions on Vehicular Technology*, vol. 64, no. 10, pp. 4839–4845, 2015.
[19] L. Liu, G. Peng, P. Wang et al., "Energy-and area-efficient recursive-conjugate-gradient-based MMSE detector for massive MIMO systems," *IEEE Transactions on Signal Processing*, vol. 68, pp. 573–588, 2020.
[20] Y. Saad, *Iterative Methods for Sparse Linear Systems*, Society for Industrial and Applied Mathematics, 2003.